Electron capture branching ratios for the odd-odd intermediate nuclei in double-beta decay using the TITAN ion trap facility

D. Frekers, J. Dilling, and I. Tanihata

Abstract: We suggest a measurement of the electron capture (EC) branching ratios for the odd-odd intermediate nuclei in double-beta ($\beta^-\beta^-$) decay using the new ion trap facility TITAN at the TRIUMF radioactive beam facility. The EC branching ratios are important for evaluating the nuclear matrix elements involved in the $\beta^-\beta^-$-decay for both, the 2ν and the 0ν-decay mode. Especially the neutrinoless ($0\nu\beta\beta$) mode is presently at the center of attention, as it probes the Majorana character of the neutrino, and if observed unambiguously, knowledge of the nuclear matrix elements are the key for determining the neutrino mass. The EC branches are in most cases suppressed by several orders of magnitude relative to their β^--counterparts owing to much lower decay energies, and are therefore either poorly known or not known at all. Here, the traditional methods of producing the radioactive isotope through irradiation of a suitable target and then measuring the K-shell X-rays have reached a limit of sensitivity. In this note we will describe a novel technique to measure the EC branching ratios, where the TITAN ion traps and the ISAC radioactive beam facility at TRIUMF are the central components. This approach will increase the sensitivity limit because of significantly reduced background levels. Seven cases will be discussed in detail and connections to hadronic charge-exchange reactions will be made. For most of these, the daughter isotopes are $\beta^-\beta^-$-decay nuclei that are presently under intense experimental investigations. These are:

^{76}As $(2^- \xrightarrow{EC} 0^+)^{76}$Ge, ^{82m}Br $(2^- \xrightarrow{EC} 0^+)^{82}$Se, ^{100}Tc $(1^+ \xrightarrow{EC} 0^+)^{100}$Mo, ^{110}Ag $(1^+ \xrightarrow{EC} 0^+)^{110}$Pd, ^{114}In $(1^+ \xrightarrow{EC} 0^+)^{114}$Cd, ^{116}In $(1^+ \xrightarrow{EC} 0^+)$ ^{116}Cd, ^{128}I $(1^+ \xrightarrow{EC} 0^+)^{128}$Te.

PACS Nos.: 23.40.-s, 23.40.Hc, 29.30.Kv, 29.25.Rm, 14.60.Pq

D. Frekers.[1] Institut für Kernphysik,
Westfälische Wilhelms-Universität, 48149 Münster, Germany, and TRIUMF, 4004 Wesbrook Mall, Vancouver, BC, V6T 2A3
J. Dilling. TRIUMF, 4004 Wesbrook Mall, Vancouver, V6T 2A3
I. Tanihata. TRIUMF, 4004 Wesbrook Mall, Vancouver, V6T 2A3

[1] Corresponding author (e-mail: frekers@triumf.ca).

 DOI: 10.1139/*Zxx-xxx*

1. General considerations

The nuclear $\beta\beta$-decay is characterized by a transition among isobaric nuclei, whereby the nuclear charge Z changes by two units. All $\beta\beta$-emitters are among even-even nuclei, and therefore the decay connects their ground-state spins and parities through a $0^+ \longrightarrow 0^+$ transition. The $\beta\beta$-transition is believed to occur in at least two different modes, the 2ν-mode and the 0ν-mode, the latter is forbidden in the Standard Model and requires the neutrino to be a Majorana particle. There are other exotic modes proposed as well, mostly connected with right-handed currents, or with additional particles like majorons, to which the neutrino can couple, or more recently with super-symmetry. All of those connect the neutrinoless $\beta\beta$-decay with other properties in particle physics, most notably with some rare and so far unobserved decays of the muon. [1–3].

1.1. The $2\nu\beta^-\beta^-$-process

The $2\nu\beta^-\beta^-$-decay process

$$(Z, A) \rightarrow (Z + 2, A) + 2e^- + 2\bar{\nu}_e$$

conserves lepton number and is allowed within the Standard Model, independent of the nature of the neutrino. This mode is a second-order weak process and therefore, the decay rate is proportional to $\left[\frac{G_F}{\sqrt{2}}\cos(\Theta_C)\right]^4$ and, consequently, lifetimes are long compared to ordinary β-decay. The decay rate is given by

$$\begin{aligned} \Gamma^{2\nu}_{(\beta^-\beta^-)} &= \frac{C}{8\pi^7}\left(\frac{G_F}{\sqrt{2}}\cos(\Theta_C)\right)^4 \mathcal{F}^2_{(-)}\left|M^{(2\nu)}_{DGT}\right|^2 f(Q) \\ &= G^{2\nu}(Q, Z)\left|M^{(2\nu)}_{DGT}\right|^2 \\ \mathcal{F}_{(-)} &= \frac{2\pi\alpha Z}{1 - \exp(-2\pi\alpha Z)}. \end{aligned} \tag{1.1}$$

Here, G_F is the Fermi constant, Θ_C is the Cabibbo angle, $\mathcal{F}_{(-)}$ is the Coulomb factor for β^--decay, α the fine structure constant and Z the atomic number of the daughter nucleus. The factor C is a relativistic correction term for $\beta^-\beta^-$-decay, which enhances the decay for high-Z nuclei (C is of order unity for $Z = 20$ and ≈ 5 for $Z = 50$). Equation (1.1) is called the Primakoff-Rosen approximation [4], which is often used to simplify the otherwise complex structure of the formula. The factor $f(Q)$ can be expressed in terms of a polynomial of order Q^{11}, where Q is the reaction Q-value. This high Q-value dependence is essentially a result of the phase space. The quantity $G^{2\nu}(Q, Z)$ is the combined phase-space factor, and values for different nuclei are summarized in Ref. [5]. Note that these values contain a slight model dependence as a result of a particular choice of the nuclear charge radius. The nuclear structure dependence is given by the $\beta\beta$-decay Gamow-Teller matrix element $M^{(2\nu)}_{DGT}$:

$$\begin{aligned} M^{(2\nu)}_{\mathrm{DGT}} &= \sum_m \frac{\langle 0^f_{g.s.}|\sum_k \sigma_k\tau^-_k\,|1^+_m\rangle\,\langle 1^+_m|\sum_k \sigma_k\tau^-_k\,|0^i_{g.s.}\rangle}{\frac{1}{2}Q_{\beta\beta}(0^{(f)}_{g.s.}) + E(1^+_m) - E_0} \\ &= \sum_m \frac{M_m\,(GT^+)\,M_m\,(GT^-)}{E_m} \end{aligned} \tag{1.2}$$

Here, $E(1^+_m) - E_0$ is the energy difference between the $\mathrm{m^{th}}$ intermediate 1^+ state and the initial ground state, and the sum $\sum_k$ runs over all the neutrons of the decaying nucleus. (Note that the insertion of $M_m\,(GT^+)$ in the second equation is the result of time invariance, also note that the energy denominator is in units of the electron rest mass m_e.) Contributions from Fermi-type virtual transitions are negligible, because initial and final states belong to different isospin multiplets. In fact, the transition matrix is essentially a sum of products of two ordinary β-decay Gamow-Teller matrix elements between the initial and the intermediate states, and between the intermediate states and the final ground state, respectively. Because in this case two real neutrinos are emitted, the intermediate states m that contribute will be 1^+ states, whose transition matrix elements can be determined e.g. through charge-exchange reactions in the β^+ and β^--direction at intermediate energies of $100-200$ MeV/nucleon [6–13] , or, for the ground-state transitions, by measuring the single (β^+ / EC) and β^--decay rates.

1.2. The $0\nu\beta^-\beta^-$-process

The $0\nu\beta^-\beta^-$-decay process

$$(Z, A) \rightarrow (Z+2, A) + 2e^-$$

is a lepton number violating process. In weak interaction gauge theories this requires the neutrino to be a massive Majorana particle irrespective of the mechanism which drives the decay [14]. Because of the helicity matching condition the decay rate is then given by:

$$\Gamma^{\,0\nu}_{(\beta^-\beta^-)} = G^{\,0\nu}(Q, Z) \left| M^{(0\nu)}_{DGT} - \frac{g_V}{g_A} M^{(0\nu)}_{DF} \right|^2 \langle m_{\nu_e} \rangle^2 \,. \tag{1.3}$$

$G^{0\nu}(Q, Z)$ is in general a more favorable phase-space factor than the one in $2\nu\beta^-\beta^-$ mode, although it scales with Q^5. The quantities $M^{(0\nu)}_{DGT}$ and $M^{(0\nu)}_{DF}$ are generalized Gamow-Teller and Fermi matrix elements for $0\nu\beta^-\beta^-$-decay, and $\langle m_{\nu_e} \rangle$ is the effective Majorana neutrino mass given as

$$\langle m_{\nu_\mathrm{e}} \rangle = \left| \sum\nolimits_i U_{\mathrm{e}i}^{\,2}\; m_i \right| \tag{1.4}$$

The $U_{\mathrm{e}i}$ are the elements of the mixing matrix containing two mixing angles θ_{12} and θ_{13} as well as two CP phases ϕ_{12} and ϕ_{13}, and m_i are the three corresponding mass eigenvalues. In order to extract the neutrino mass from an observed decay rate, the nuclear matrix elements need to be known with some reasonable reliability. Whereas the matrix elements in the $2\nu\beta\beta$-decay have a rather simple structure, the ones for the $0\nu\beta\beta$-decay are significantly more complex, since the neutrino enters into the description as a virtual particle. Usually, the generalized matrix elements are expressed in terms of a neutrino potential operator (cf. Refs. [5, 15–17] and references therein):

$$M^{(0\nu)}_{DGT} = \langle f | \sum_{lk} \sigma_l \sigma_k \tau^-_l \tau^-_k H_{GT}(r_{lk}, E_a) \, | i \rangle \tag{1.5}$$

$$M^{(0\nu)}_{DF} = \langle f | \sum_{lk} \tau^-_l \tau^-_k H_F(r_{lk}, E_a) \, | i \rangle \,, \tag{1.6}$$

where r_{lk} is the proton-neutron distance in the nucleus, and E_a is an energy parameter related to the excitation energy. (Note that short-range effects become important here.) As the distance r_{lk} is of order the size of the nucleus, the momentum transfers involved can be large, typically of order $0.5 fm^{-1}$,

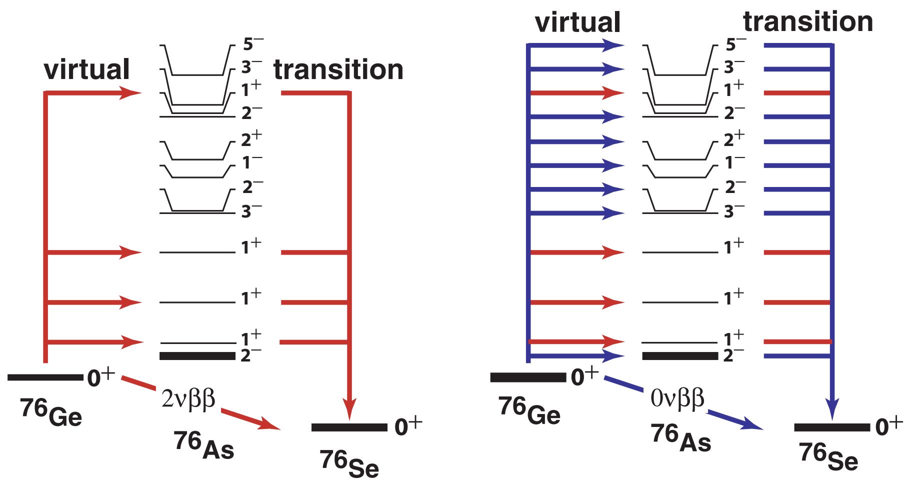

Fig. 1. Sketch of the two modes of $\beta^-\beta^-$-decay and the various possible excitations of the intermediate nucleus. (Note that except for the ground states, all other state properties are indicative only.)

which then allows excitation of many intermediate states. After a multipole expansion of Eqs.(1.5) and (1.6), one can re-write the general structure of Eq.(1.3) in the following way:

$$\begin{aligned}\Gamma^{0\nu}_{(\beta^-\beta^-)} &= G^{0\nu}(Q,Z) \\ &\times \left| \sum\nolimits_m \frac{\langle 0^f_{g.s.} | \, |\mathcal{O}_{\sigma\tau^-}(r,S,L)| \, | J^\pi_m \rangle \, \langle J^\pi_m | \, |\mathcal{O}_{\sigma\tau^-}(r,S,L)| \, | 0^i_{g.s.} \rangle}{\frac{1}{2} Q_{\beta\beta}(0^{(f)}_{g.s.}) + E(J^\pi_m) - E_0} + \text{Fermi} \right|^2 \langle m_{\nu_e} \rangle^2 \quad (1.7)\end{aligned}$$

The two different situations of $\beta\beta$-decay are sketched in Fig.1. Clearly, an experimental determination of all matrix elements involved in the $0\nu\beta\beta$-decay case is an insurmountable task, unless one could show that low-lying states of lowest multipolarity (e.g. $J^\pi = 1^+, 2^-, 3^+$) were the main contributors to the rates factor. Some theoretical models seem to indicate this [18, 19].

1.3. Description of theoretical approaches and the problem of g_{pp}

In this section, we briefly review some of the theoretical work connected with the determination of $\beta^-\beta^-$-decay matrix elements. The theoretical models that are being applied usually employ the Quasi-particle Random-Phase-Approximation (QRPA) as a basis [18–27]. The QRPA is an intrinsically collective model, and as such, it has been overwhelmingly successful in describing collective properties of nuclei in a mass region, where a shell-model treatment presently reaches a limit (i.e. around $A \approx 70$). In applying the concept of the QRPA to the $\beta^-\beta^-$-decay nuclear matrix elements, some universal features seem to emerge (Refs. [18, 19]), namely the dominance of a few low-lying nuclear states of low multipolarity (like e.g. the 2^- states, which could exhaust nearly 50% of the total summed strength in $0\nu\beta^-\beta^-$-decay). On the other hand, the authors of Ref. [18] also point out that there is a worrisome inability to correctly describe the single decay rates (like the β^-, and most notably the EC rate where available). It is argued that the theoretical agreement with the experimental $2\nu\beta^-\beta^-$-decay rate is a result of two compensating errors, much too high an EC rate and a too low β^- rate. Discrepancies of 1 to 2 orders of magnitude in the EC matrix elements are possible, and since the understanding and correct description of the $2\nu\beta^-\beta^-$-process is a pre-requisite for the description of the $0\nu\beta^-\beta^-$-decay,

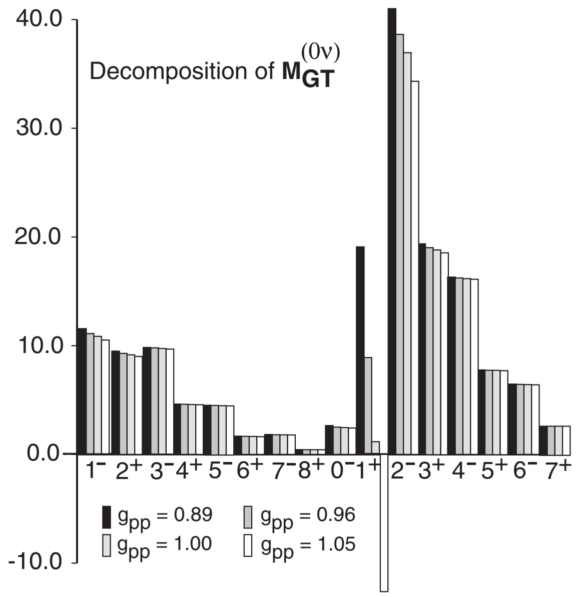

Fig. 2. Decomposition of the ^{76}Ge$\longrightarrow^{76}$Se $0\nu\beta^-\beta^-$-decay matrix elements into multipole components for various values of g_{pp} parameters. The components are separated into natural and unnatural parity parts. (From Refs. [19, 28])

one could be forced to re-evaluate many of the models that have so far been advocated. Unfortunately, EC decay branches are in many cases either not well enough known, or not known at all, contrary to the β^--decay branches, which have been measured with high precision. This means, there is presently a rather uncomfortable loose end in the theoretical models.

In fact, the $2\nu\beta^-\beta^-$-decay is always used as a test case for a nuclear model, since the decay proceeds via the 1^+ states of the intermediate nucleus only. Here the proton-neutron-QRPA (pn-QRPA) model is being employed, which is designed for spherical or near-spherical nuclei. The pn-QRPA has an adjustable particle-particle parameter part of the proton-neutron two-body interaction, called g_{pp}. The parameter appears in all single and double-beta decay calculations and defines part of the nuclear many-body Hamiltonian. It turns out that the nuclear matrix elements of the $2\nu\beta^-\beta^-$-decay seem to be rather sensitive to g_{pp}, which requires this parameter to be tuned by this decay. This is, in fact, the procedure followed by all theoretical groups, i.e.: the interaction strength parameter g_{pp} of the pn-QRPA is determined by fitting the computed nuclear matrix elements of Eq.1.2 to the one extracted from the experimental half-life of the corresponding $2\nu\beta^-\beta^-$-decay. This fitted value is then used for the evaluation of the $0\nu\beta^-\beta^-$-decay matrix elements of Eq.1.7, which, contrary to the 2ν case, seem to be rather insensitive to g_{pp}, with only the 1^+ transition matrix element being a marked exception. Thus, one could be tempted to conclude that the $0\nu\beta^-\beta^-$-decay is well controlled by the theory, if one assumes, of course, that the energy denominator in Eq.1.7, which contains the excitation energy, is equally well understood. In Fig.2 this situation is depicted for the case of ^{76}Ge$\longrightarrow^{76}$Se. As, however, pointed out in Ref. [18], there are pitfalls in this procedure casting serious doubts on the usefulness of the method and the universal parameter g_{pp}. The inadequacies of the model become apparent when confronting it with the single decays, most notably with EC rates, where available.

In the following we discuss three examples, ^{116}Cd, ^{128}Te, and ^{76}Ge. We make use of the results of calculations from Refs. [18, 19] and also follow a similar discussion presented there.

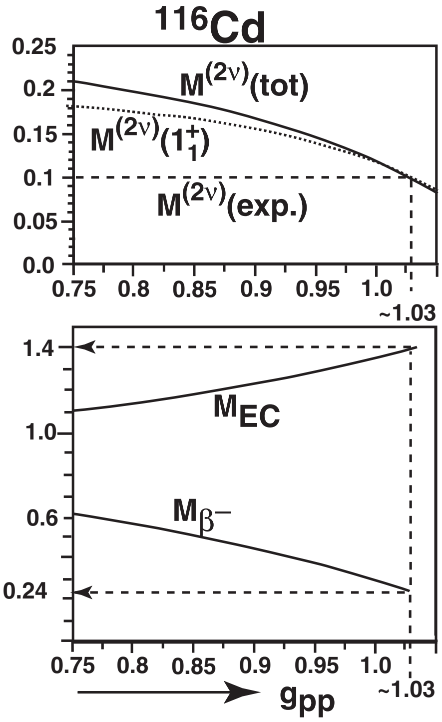

Fig. 3. Nuclear matrix elements for ^{116}Cd $\beta^-\beta^-$decay as a function of the parameter g_{pp}. The top part shows the $2\nu\beta^-\beta^-$-decay matrix elements for the full calculation ($M^{(2\nu)}_{tot}$) (full line), the contribution from the first 1^+ state, i.e. ground state (dashed line), and the extracted experimental value, which fixes g_{pp}. The lower part shows the extracted single decay matrix elements as a function of g_{pp}. (Taken from Ref. [18]

In fact, the situation is best illustrated in the case of ^{116}Cd. The calculations of the $2\nu\beta^-\beta^-$-decay matrix elements have been performed on the basis of the pn-QRPA (for more information about the details of the calculations, we refer to Ref. [5]). The results are summarized in Fig.3. Following the above indicated recipe of fixing the parameter g_{pp}, one has to compare the total $2\nu\beta^-\beta^-$-decay matrix element $M^{(2\nu)}_{tot}$ of Eq.1.2 with the one evaluated from the experimental half-life $M^{(2\nu)}(\mathrm{exp})$. From this a value of $g_{pp} = 1.03$ is deduced. Also indicated in Fig.3 is the contribution of the lowest-lying 1^+ state, which coincides with the ground state. It thus appears that near $g_{pp} = 1$ the nuclear matrix element for the 1^+ ground state coincides with the total value of the matrix element. This is a characteristic of the so-called single-state-dominance (SSD). Although the extreme SSD model may not be realistic, as recently shown by comparing the charge-exchange reactions (^{3}He, t) and (d,^{2}He) on the A=116 system (cf. Ref. [7]), it is nevertheless instructive to follow up the consequences. In the case of an SSD (or an approximate SSD), the nuclear matrix element of the $2\nu\beta^-\beta^-$-decay of Eq.1.2 simplifies to:

$$M^{(2\nu)}_{tot} \simeq \frac{M_{EC}M_{\beta^-}}{\frac{1}{2}Q_{\beta\beta}(0^{(f)}_{g.s.}) + E_{g.s.}(1^+) - E_0} \tag{1.8}$$

where M_{EC} is the electron capture branch and M_{β^-} is the single β^--decay branch. As g_{pp} also appears in the single β^--decay calculations, the model makes a prediction for the single β^--decay and thereby for the EC decay branch as well. This is indicated in the lower part of Fig.3. Theory can therefore already at this stage be confronted with experiment.

The value of $g_{pp} = 1.03$, as required by the experimental $2\nu\beta^-\beta^-$-decay half-life, gives for the single β^--decay matrix element a value of $M_{\beta^-} = 0.24$ and for the EC matrix element a value of $M_{EC} = 1.4$. The experimental value for the β^--decay is, however, $M_{\beta^-} = 0.51$, as determined from the ^{116}In half-life ($T_{1/2} = 14.10 \pm 0.03$ s) and its $logft = 4.65$. A matrix element of $M_{\beta^-} = 0.24$ would slow down this transition to $T_{1/2} \approx 63$ s. However, one could re-adjust the parameter to $g_{pp} = 0.85$ to match the experimental β^--decay matrix element using as an argument the experimental error of the $2\nu\beta^-\beta^-$-decay half-life. In this case, the EC matrix element decreases from $M_{EC} = 1.4$ to a slightly more favorable value of $M_{EC} = 1.2$. The experimental value for the EC matrix element is, however, $M_{EC} = 0.18$ (as deduced from (^{3}He, t) charge-exchange reactions [29]) or $M_{EC} = 0.63$ (as deduced from a direct measurement using the conventional technique of detecting the K-shell X-rays after irradiation [30], see also Appendix A). These different values have a dramatic effect on the EC branching ratio ε (for the β^--decay branch we use the experimental value):

- $M_{EC} = 1.4/1.2$ translates into $\varepsilon = 0.115/0.083\%$ ($logft = 3.77/3.91$) (theory, Ref. [18])
- $M_{EC} = 0.18$ translates into $\varepsilon = 0.0019\%$ ($logft = 5.5$) (expmt-1, Ref. [29])
- $M_{EC} = 0.63$ translates into $\varepsilon = 0.023\%$ ($logft = 4.47$) (expmt-2, Ref. [30])

Clearly, none of the experimental values for ε can be made consistent with the g_{pp} dependence shown in Fig.3. Therefore, one may summarize: The use of $g_{pp}(\beta\beta) = 1.03$ reproduces the $2\nu\beta^-\beta^-$-decay half-life via a conspiracy of two errors: a much too large EC matrix element (too fast EC decay) is compensated by a much too small β^--decay matrix element (too slow β^--decay).

A comment on the contradicting experimental values for the EC branch is also in order:

The EC branching ratio for the $^{116}\text{In} \xrightarrow{EC} {}^{116}\text{Cd}$ has recently been measured by Bhattacharya, et al. [30] at the Notre Dame FN Tandem Accelerator using the $^{115}\text{In}(d,p)$ reaction for ^{116}In production. A He-jet system was used to transport the radio-isotope away from the production onto a tape station, where the X-ray detection system was located. The authors report a branching ratio $\varepsilon = (0.0227 \pm 0.0063)\%$, which translates into $log\ ft = 4.47^{(+0.14)}_{(-0.10)}$, $B(GT) = 0.39 \pm 0.1$, and $M_{EC} = 0.63 \pm 0.09$. These values are at variance with a recent measurement at RCNP of the $^{116}\text{Cd}(^3\text{He},t)^{116}\text{In}$ charge-exchange reaction at 450 MeV [29], where it was observed that the ground-state transition was only weakly excited. Here, the corresponding values were: $log\ ft = 5.56^{(+0.07)}_{(-0.06)}$, $B(GT) = 0.032 \pm 0.005$, and $M_{EC} = 0.18 \pm 0.015$. Of course, one could argue that the proportionality between $B(GT)$ and the $(^3\text{He},t)$ charge-exchange cross section is not safely established [31], but such a large discrepancy factor (here a factor of 12 for the $B(GT)$ values) would be exceptional, especially since the EC $log\ ft$-value indicates a rather low degree of forbiddeness, which ought to translate into a rather strong charge-exchange transition. On the other hand, for a number of neighboring nuclei also investigated by Akimune et al. [29], like ^{118,120}Sb and ^{112}In, there is a high degree of consistency between $B(GT)$ values deduced from β^+-decay and those deduced from $(^3\text{He},t)$ charge-exchange reactions on ^{118,120}Sn and ^{112}Cd. We may also refer to a recent publication, where this issue and its consequences for $\beta^-\beta^-$-decay are discussed in the context of the $(d,^2\text{He})$ charge-exchange reactions performed at the KVI Groningen [7].

In view of the general importance connected with $\beta^-\beta^-$-decay, the particular situation around the ^{116}In weak decay is rather disconcerting. Not only are there serious deficiencies being exposed in the theory, but the experimental situation as well is equally uncomfortable.

As the second test case one can take the $2\nu\beta^-\beta^-$-decay of ^{128}Te to the ground state of ^{128}Xe. The intermediate nucleus is ^{128}I with a ground-state spin $J^\pi = 1^+$. This case can be analyzed in much the same way as indicated above, and we refer to Ref. [18], where it is discussed in detail and where similar

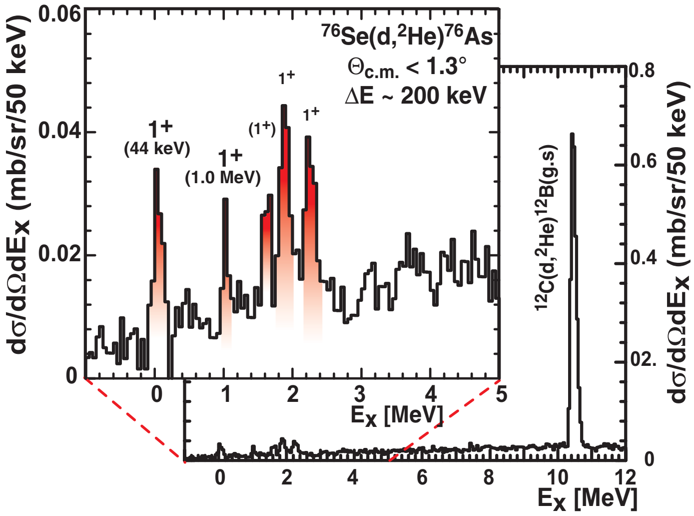

Fig. 4. Spectrum of the charge-exchange reaction $^{76}\mathrm{Se}(d,^{2}\mathrm{He})^{76}\mathrm{As}$ at 183 MeV incident energy showing the excitation energy spectrum of ^{76}As up to 12 MeV. As carbon has been used as a target backing material, the $^{12}\mathrm{C}(d,^{2}\mathrm{He})^{12}\mathrm{B}$ ground-state reaction appears at about 10.46 MeV in the frame of the ^{76}As excitation energy owing to the different Q-values involved. The low excitation energy is enlarged to show the levels of ^{76}As. The Gamow-Teller transition strengths are related to the matrix elements for the β^--decay direction.

conclusions to the ones above are drawn: The matrix elements extracted for the two branches, i.e. the EC and the β^--decay, cannot be brought together with a single g_{pp} value. The g_{pp} value that fits the $2\nu\beta^-\beta^-$-decay would lead to a much too fast EC rate and a much too slow β^--rate. A re-adjustment of g_{pp} to the experimental β^--decay does not notably improve the EC rate prediction. It would still be almost one order of magnitude to fast.

The third case, the $\beta^-\beta^-$-decay of ^{76}Ge to ^{76}Se can also be discussed along the same lines. ^{76}Ge can be considered the most important case, because of the recent claim for an observation of the 0ν-decay mode [32]. The intermediate nucleus, ^{76}As, has a 2^- ground state, which undergoes a weak first-order unique transition by β^--decay and by electron capture. Apart from the fact that this provides an important opportunity to determine the matrix element for the next hierarchy up in multipolarity, i.e. the matrix element, which is most relevant to $0\nu\beta^-\beta^-$-decay, it is nevertheless instructive to comment on the structure of the low-lying 1^+ levels in the context of g_{pp}. As a result of our on-going effort to use charge-exchange reactions to determine nuclear matrix elements, we have recently completed a measurement of the $(d,^{2}\mathrm{He})$ charge-exchange reactions, where the transition strength $B(GT^+)$, which is the quantity that connects to the β^--decay, was extracted. The spectrum is shown in Fig.4. The first 1^+ level is only 44 keV above the ground state and carries a strength of $B(GT) \approx 0.14$, which translates into a matrix element of a hypothetical β^--decay, $M_{\beta^-} \approx 0.37$. A g_{pp} value that fits the $2\nu\beta^-\beta^-$ decay ($g_{pp} = 0.95$) would result in $M_{\beta^-} = 0.09$. Again, we see that even for the excited states, the β^--decay branch determined by theory is too slow by more than an order of magnitude.

2. Details of the ground-state decay properties of the odd-odd intermediate nuclei

In this section we will provide detailed information about the various isotopes in question. It is envisaged that we will use the TITAN ion trap facility to capture the radioactive ions and detect the X-ray transitions with high-resolution X-ray detectors. The power of the trap technique lies in its ability to provide largely a background-free situation for low-energy X-ray detection by storing a mass selected mono-isotopic sample in an electro-magnetic field. Further, there will be no X-ray absorption, which one would typically have to deal with when implanting the isotope into/onto some carrier material. Electrons from the far more intense β^--decay will be guided away from the X-ray detectors by the high magnetic field (magnetic field strength 6 T) of the trap and can be detected on the beam axis when exiting the magnet. This provides an additional (soft) anti-coincidence gate, which can be used to gate on unwanted X-rays associated with the β^--decay.

K-shell X-ray energies will typically lie between 10 and 30 keV, and high-resolution X-ray detectors will provide additional information about the K/L capture ratio. This may be another important quantity to test details of the electronic wave function. The fluorescence yields ω_K are known to high precision ($\Delta\omega_K/\omega_K < 3\%$) for all nuclei involved. Typical values as taken from the compilation of Krause [33] for the Ge and Se nuclei are about 55% and 60% and for the other higher mass nuclei between 77% and 87%.

With a few exceptions, all nuclei discussed here are at the center of experimental $\beta^-\beta^-$-decay experiments. There are at least 5 nuclei, whose atomic masses are close to each other, allowing theoretical models to be tuned without too much of a different nuclear structure involved. Half-lives of all intermediate nuclei are short enough as to not cause serious contamination of any of the equipment used.

2.1. The case ^{100}Tc

The intermediate nucleus in the ^{100}Mo $\beta^-\beta^-$-decay is ^{100}Tc (cf. Fig.5a). Its half-life is 15.8 s. The EC decay will only populate the ground state of ^{100}Mo, as there are no excited states below 168 keV in ^{100}Mo. The EC ratio has been measured by García et al. [34] to $\varepsilon = (1.8 \pm 0.9) \cdot 10^{-3}\%$, which translates into a $log ft = 4.44^{+0.30}_{-0.18}$ and a $B(GT) = 0.42 \pm 0.21$. The large error makes this value consistent with the one measured through the (^{3}He, t) charge-exchange reaction by Akimune at al. [29], which is $B(GT) = 0.33 \pm 0.04$.

The β^--decay of ^{100}Tc has a 93% branch to the ground state ($log\ ft = 4.60$) and a 5.7% branch to a 1.130 MeV (0^+) state in ^{100}Ru [36]. There are a number of other weak transitions (mostly below 0.1%), all of them producing γ-rays at significantly higher energies than the typical X-ray energies. Internal conversion (IT) coefficients are not known and although they are likely small, the internal conversion branches could compete in magnitude with the EC branch, thereby producing K-shell X-rays at 19.3 keV in ^{100}Ru compared to the 17.5 keV ones accompanying the EC decay to ^{100}Mo. High-resolution spectroscopy is therefore always imperative.

A ^{100}Mo $\beta^-\beta^-$-decay experiment is presently being set up by the MOON collaboration [35] as a follow-up of the previous ELEGANT-V experiment [37,38] using ≈ 1 t of ^{100}Mo. This is a significant increase in mass compared to the ≈ 7 kg of ^{100}Mo used by the NEMO-3 collaboration [39,40]. NEMO-3 recently reported a high precision life-time value for $2\nu\beta^-\beta^-$-decay ($T_{1/2}(2\nu\beta\beta) = [\ 7.11 \pm 0.02\,\mathrm{stat} \pm 0.54\,\mathrm{syst}\ ] \cdot 10^{18}\mathrm{yr}$), but only a lower limit for the $0\nu\beta^-\beta^-$-decay time ($T_{1/2}(0\nu\beta\beta) > 4.6 \cdot 10^{23}\mathrm{yr}$). This lower-limit value translates into an upper limit for the effective mass of the Majorana neutrino of $m_\nu < 0.7 - 2.8$ eV [40]. The large spread in the upper limit of the mass is entirely due to the poor convergence of the various theoretical models dealing with nuclear matrix elements [21,23,24,41,42].

Besides the possibility to study the $\beta^-\beta^-$-decay, the MOON collaboration will also exploit ^{100}Mo for measuring the solar neutrino flux through the charged-current $^{100}\mathrm{Mo}(\nu, \mathrm{e}^-)^{100}\mathrm{Tc}$ reaction using the subsequent delayed β^--decay of the short-lived ^{100}Tc as a neutrino flux indicator, and, by the same reaction, to observe the neutrino flux from a supernova explosion, if such an event were to happen in our Galaxy in the near future. In all these cases, the EC matrix element is an essential piece of information for determining absolute values for neutrino fluxes. Because of its recognized importance, the EC

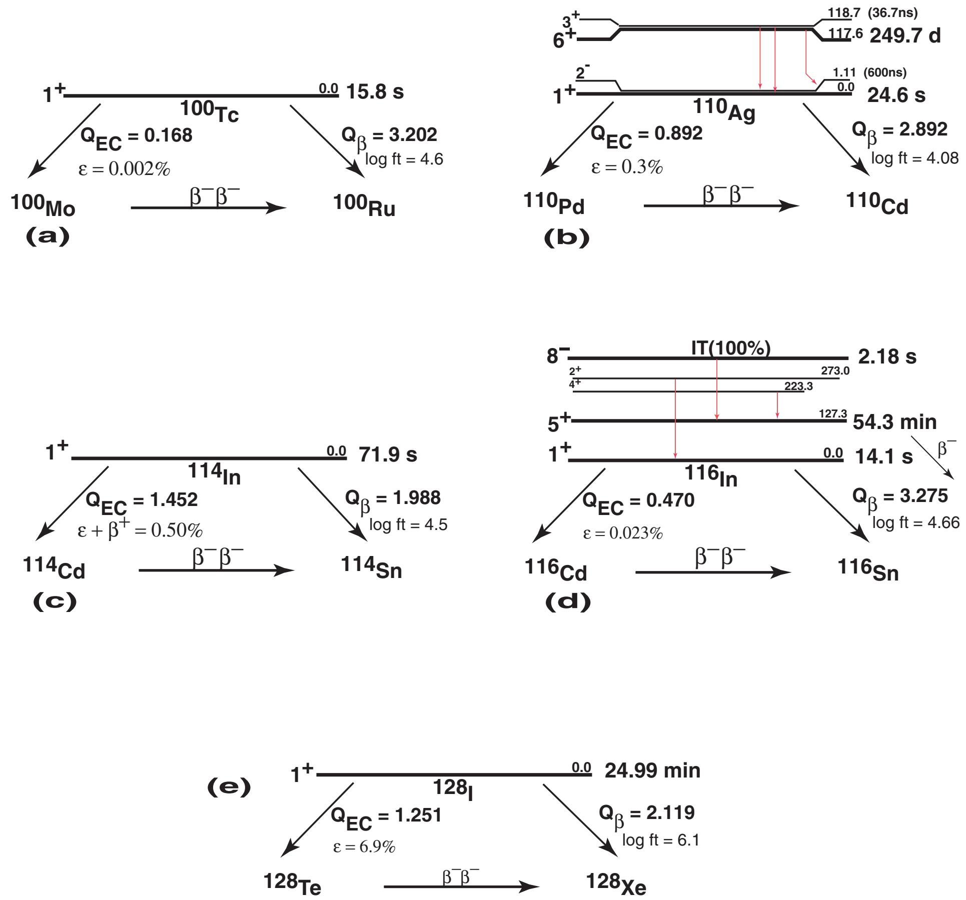

Fig. 5. Decay scheme of ^{100}Tc, ^{110}Ag, ^{114}In, ^{116}In and ^{128}I showing also their lowest-lying isomeric states.

decay of the ^{100}Tc isotope has recently been investigated by a group of the University of Washington [43] using the IGISOL radioactive isotope facility at Jyväskylä, Finland. However, here the traditional technique that was also used in the previous experiment of Ref. [34], i.e. catching the isotope onto a tape station, was employed. The preliminary result communicated in Ref. [43] is presently at variance with the results from a (^{3}He, t) charge-exchange measurement performed at RCNP [29, 44], but also with the previous value from García et al. [34].

2.2. The case ^{110}Ag

The intermediate nucleus in the ^{110}Pd $\beta^-\beta^-$-decay is ^{110}Ag (cf. Fig.5b). Its half-life is 24.6 s. This nucleus has a 249.7 d, $J^\pi = 6^+$ isomeric state at 117.6 keV, which mainly decays via β^--emission (98.6%). There is a 1.36% internal conversion (IT) branch producing a 22.2 keV X-ray of ^{110}Ag. A de-excitation of the isomeric state through EC is not possible by angular momentum considerations. The ground-state EC branching ratio has been measured in 1965 [47] through production of ^{110}Ag by neutron activation. The EC branching ratio of $\varepsilon = (0.3 \pm 0.06)\%$ translates into a $log\ ft = 4.1 \pm 0.1$. Electron capture to an excited $J^\pi = 2^+$ state at 374 keV in ^{110}Pd has not been observed; its branch will likely be at least an order of magnitude lower than that to the ground state.

The β^--decay populates the ground state of ^{110}Cd with a 94.9% branch and the first excited 2^+ state at 657.8 keV at a level of 4.4%. The 249.7 d isomer decay populates high-lying high-spin states in ^{110}Cd.

There is only limited interest in using ^{110}Pd for $\beta^-\beta^-$-decay experiment and no such experiment is planned. A re-measurement of the EC branching ratio is nonetheless important for providing consistency of theoretical models in this mass range.

2.3. The case ^{114}In

The intermediate nucleus in the ^{114}Cd $\beta^-\beta^-$-decay is ^{114}In (cf. Fig.5c). Its half-life is 71.9 s. It has a 49.51 d, $J^\pi = 5^+$ isomeric state at 190.3 keV, which decays with 95.6% via an internal conversion and with 4.3% via a combined (β^+ + EC) transition.

The EC branching ratio has been measured in 1956 by Frevert et al. (Ref. [48], but see also Ref. [45]) to $BR(\mathrm{EC} + \beta^+) = (0.5 \pm 0.15\%)$, which translates into a $log\ ft = 4.9 \pm 0.2$, if there is exclusive decay into the ground state (note that the β^+ branch can be calculated to be about 0.75% of the EC branch [49]). Because of the high Q-value, the EC decay can reach a number of excited states in ^{114}Cd , most notably the first excited 2^+ state at 558.4 keV and the 0^+ state at 1134.5 keV. The sum of these branching ratios does not exceed 0.08% [45].

The β^--decay populates the ground state of ^{114}Sn with a 98.9% branch and the first excited 2^+ state at 1.300 MeV at a level of 0.14% [45].

2.4. The case ^{116}In

The intermediate nucleus in the ^{116}Cd $\beta^-\beta^-$-decay is ^{116}In (cf. Fig.5d). Its half-life is 14.1 s. It has a 54.3 min, $J^\pi = 5^+$ isomeric state at 127.3 keV, which decays predominantly (measured to be at 100%) through β^--emission populating high-lying high-spin states in ^{116}Sn. Further, there is a 2.18 s, $J^\pi = 8^-$ isomer at 289.7 keV, which decays via internal conversion only. The β^- ground-state decay branch populates the ground state of ^{116}Sn at a level of 98.6%, thereby giving a $logft$ value of 4.66 [46].

The present ^{116}Cd ground-state EC branching ratio of $\varepsilon = (0.023 \pm 0.006)\%$ [30] is, as indicated earlier, in direct conflict with the value $\varepsilon = (0.0019 \pm 0.0003)\%$ deduced from the (^{3}He,t) charge-exchange reaction [29]. In view of the importance to $\beta^-\beta^-$-decay, a novel approach to the measurement of the EC decay is clearly warranted to resolve this discrepancy. In doing so, special care has to be taken to discriminate the isomeric decays using their different decay times.

2.5. The case ^{128}I

The intermediate nucleus in the ^{128}Te $\beta^-\beta^-$-decay is ^{128}I (cf. Fig.5d). Its half-life is 24.99 min. There are no long-lived isomers to be considered. The (EC + β^+) branching ratio has been measured with high precision to $(6.8 \pm 0.8)\%$ [50, 51] giving a $log\ ft = 5.1$. The Q-value allows a transition into the first excited 2^+ state at 743.2 keV. Its branch is $\varepsilon = 0.16\%$ ($log\ ft = 6.0$).

The β^--decay branch populates the ground state of ^{128}Xe (80%, $log\ ft = 6.1$), the first 2^+ state at 442.9 keV (11.6%, $log\ ft = 6.5$) and the second 2^+ state at 968.5 keV (1.5%, $log\ ft = 6.7$). The nucleus ^{128}I is one of the few cases, where the EC decay is known with high precision. The decay of the nucleus ^{128}I is therefore ideally suited for testing the technique of using ion traps to measure capture ratios and for using the decay as a calibration standard.

The above mentioned isotopes, ^{114}Cd, ^{116}Cd and ^{128}Te are three of a total of nine $\beta\beta$-decaying nuclei being investigated by the COBRA collaboration [52]. COBRA uses a specially designed semiconductor crystal detector, CdZnTe, which, apart from the nuclei mentioned above, also contains the $\beta^-\beta^-$-decaying nuclei ^{70}Zn and ^{130}Te and furthermore, four additional nuclei, which can undergo a $\beta^+\beta^+$ or a combination of β^+ and EC decay (^{64}Zn, ^{106}Cd, ^{108}Cd, and ^{120}Te). The experiment

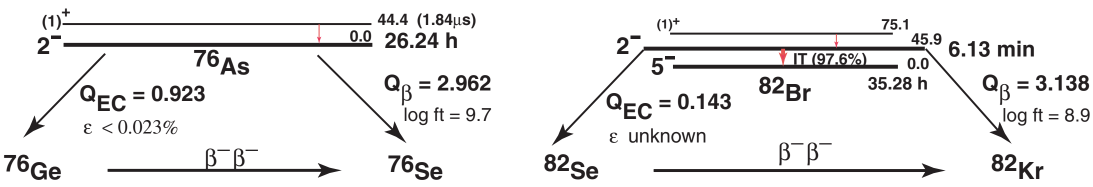

Fig. 6. Decay scheme of ^{76}As and ^{82}Br showing also their lowest-lying 1^+ levels and isomeric states.

CUORE [53] (the successor of CUORICINO), on the other hand, will focus on the $\beta^-\beta^-$-decay of ^{130}Te only and will eventually use 750 kg TeO_2 crystals operating as a cryogenic bolometer. The nucleus ^{130}Te has the largest $\beta^-\beta^-$-decay Q-value among the tellurium isotopes, however, there is a significant difference to the other isotopes, as in this case the intermediate nucleus ^{130}I has a rather high ground-state spin of $J^\pi = 5^+$. Furthermore, there is a 9.0 min, $J^\pi = 2^+$ isomer at 40 keV, which decays by internal conversion (84 %) to the ground state of ^{130}I and by β^--decay (16 %) to exited states in ^{130}Xe. A weak decay either by β^--decay or by EC to the ground states of ^{130}Xe or ^{130}Te, has a high degree of forbiddeness and so far has not been observed. On the other hand, both states, the $J^\pi = 5^+$ ground state and the $J^\pi = 2^+$ isomeric state of ^{130}I, are only of minor relevance to the overall $\beta^-\beta^-$-decay matrix element, leaving presently only charge-exchange reactions as a means to elucidate the more relevant nuclear structure involved in this decay.

2.6. The case ^{76}As

Figure 6a shows the decay scheme of ^{76}As, which is the intermediate nucleus of the ^{76}Ge $\beta^-\beta^-$-decay. The β^-decay of ^{76}As to the ground state of ^{76}Se is a first-order unique forbidden $2^- \longrightarrow 0^+$ decay (branch of 51%), whose $log\ ft = 9.7$ happens to be exceptionally large. The β^--decay also populates the first 2^+ state at 559.1 keV with a branch of 35.2% ($log\ ft = 8.1$). The rest of the decay is distributed over many levels.

Presently, only an upper limit of the EC rate is known, $\varepsilon < 0.023\%$, which originates from a 1957 measurement [54]. The Q-value of the decay allows a transition to the first excited 2^+ state at 562 keV and it could be important to distinguish this transition from the ground-state transition.

Taking a $logft$-value for the EC process similar to the one from β^--decay, one could estimate the branching ratio to be between $\varepsilon \approx 0.01\%$ ($logft \approx 9.1$) and $\varepsilon \approx 0.002\%$ ($log\ ft \approx 9.7$), which is not too far off the present upper limit. Any of these values are in reach using the present TITAN ion trap facility, although measuring times would be tens of days rather than a few hours.

^{76}Ge is presently considered the most important $\beta^-\beta^-$-decaying nucleus. This is the only nucleus, for which a signature for $0\nu\beta\beta$-decay has so far been reported [32, 55]. The positive report has prompted two new efforts GERDA and MAJORANA, which will put this observation to a serious test [56, 57]. Both experiments expect to increase the sensitivity level by about 2 orders of magnitude compared to the previous experiment. This constitutes an enormous challenge and both experiments are staged over several phases, which may also require a search for an underground laboratory with much more reduced background levels compared to the existing ones, and the presently discussed SNOLAB project [58] could well be a viable option. Clearly, if a positive result is found, one wishes to extract the mass of the Majorana neutrino with as little theoretical uncertainty as possible. The intermediate nucleus ^{76}As provides the opportunity to directly measure the matrix element for the intermediate 2^- excitation and thereby allows a much more sensitive test for the theoretical models. This is especially true, if there is a single-state dominance. Further, as indicated before, the first 1^+ level, which is only 44 keV above the ground state (cf. Fig. 4), is another key test candidate, which is presently being investigated using charge-exchange reactions like $(d,{}^2\mathrm{He})$ and $({}^3\mathrm{He},t)$ at the KVI and at RCNP. Measuring the EC rate, and complementing this with Gamow-Teller transitions to 1^+ states could provide a rather complete picture of the properties of the intermediate states in the $\beta^-\beta^-$-decay of ^{76}Ge.

2.7. The case ^{82m}Br

Figure 6b shows the decay scheme of ^{82}Br, which is the intermediate nucleus in the ^{82}Se $\beta^-\beta^-$-decay. It has a 5^- ground state, which decays predominantly into a 4^- excited state in ^{82}Kr. The ground state is of little importance for the $\beta^-\beta^-$-decay, much in contrast to the first 2^- isomeric state at 45.9 keV. As indicated earlier, 2^- excitations can be the largest contributors to the $0\nu\beta^-\beta^-$ matrix element, especially if a single-state dominance (or ”near-single-state dominance”) case prevailed. The 2^- state decays with 97.6% through internal conversion and with 2.4% by β^--emission. The 0^+ ground state of ^{82}Kr is then populated with an 88% probability, by which a $log\ ft = 8.9$ has been deduced.

A measurement of the EC rate is in this case a significant challenge. Given the Q-value, the estimated branching ratio will be about $\varepsilon \approx 5 \cdot 10^{-8}\%$ for a $logft$-value that is similar to the β^--decay. It requires an increase of the loading capacity of the trap to at least a few times 10^6 ions, before a measurement could be envisaged.

Measuring the K-shell X-ray emission may further be hampered because of the overwhelming near-by X-ray component of ^{82}Br from the internal conversion of the 2^- level. A different technique, by which the daughter could be expelled from the trap and then counted (thereby avoiding the detection of X-rays) is presently under discussion.

Besides the ^{100}Mo isotope, the NEMO-3 collaboration has also measured the ^{82}Se $\beta^-\beta^-$-decay, although with a reduced mass of only ≈ 1 kg [40]. The half-life for the $2\nu\beta^-\beta^-$-decay was reported to be $T_{1/2}(2\nu\beta\beta) = [9.6\pm0.3\ \mathrm{stat}\pm1.0\ \mathrm{syst}]\cdot10^{19}\mathrm{yr}$ and a lower limit for the one of the neutrinoless mode was given as $T_{1/2}(0\nu\beta\beta) > 1.0 \cdot 10^{23}\mathrm{yr}$, which transforms into an upper limit for the neutrino mass of $m_\nu < 1.7 - 4.9$ eV. The spread depends once again on the theoretical model used for evaluating the nuclear matrix elements [21, 23, 24, 41, 42, 59]. NEMO-3 will lower the limits on the neutrino mass from both experiments by roughly a factor of $2 - 3$ after 5 years of running time [40]. This adds importance to both, a timely experimental determination of the first-order unique forbidden EC rate of ^{82m}Br, and to a significant improvement of theoretical models dealing with the underlying nuclear physics.

3. Description of the experimental technique

Measurements of EC branching ratios are usually carried out using a conventional tape-station technique. Here the mass selected beam is deposited onto a backing material of a tape, which can be moved quickly in front of a detector assembly. The technique has a number of drawbacks in cases where transitions are weak or of low energy. There is always the issue of X-ray absorption of the backing material onto which the isotope was implanted. In addition, as the presently discussed nuclei also decay in the β^- direction, one always has to deal with an intense background from the associated β^--particles. Furthermore, the purity of the sample is quite often difficult to verify and contamination cannot be excluded. The presently proposed approach of using ion traps is novel in a number of ways. An isotopically pure sample is stored in the backing-free environment of the trap and then the X-rays following EC are observed with a high-resolution detector perpendicular to the axis of the magnet. Electrons from the associated β^--decay are guided on the magnetic field lines and focused to the center of the magnet near the exit. Because of the high field (6T), they will not reach the X-ray detectors. Another and rather unique advantage of the present EBIT trap is its open access for X-ray detectors. A total of 7 detectors can be mounted subtending 2.1% of the 4π solid angle in the present configuration.

In the following, the experimental procedure will be described in detail:

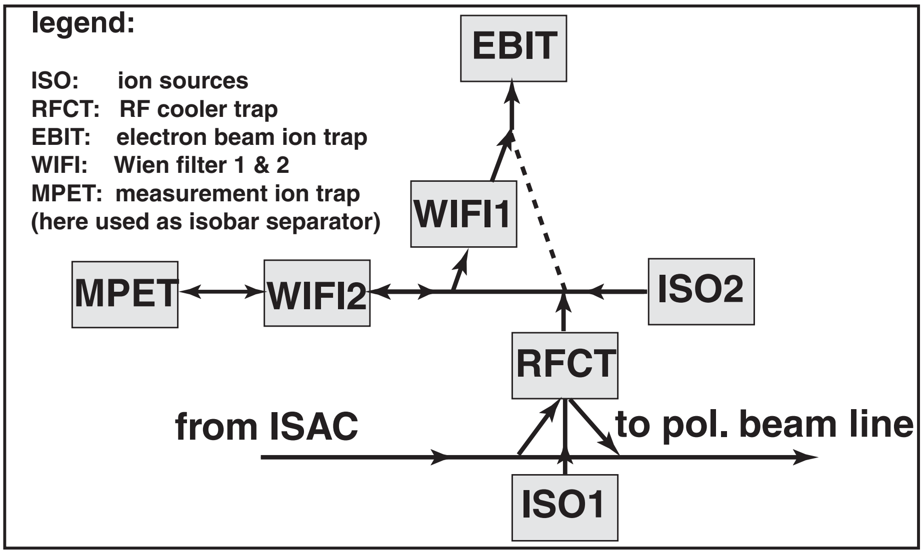

Fig. 7. The TITAN setup. Note, that the proposed configuration for the present project is slightly different from the one used for mass measurements. The beam preparation sequence is indicated with arrows.

The TITAN (TRIUMF's Ion Trap for Atomic and Nuclear physics) experimental setup is located at the ISAC radioactive on-line facility at TRIUMF. It consists of initially three ion traps in series: a linear RFQ cooler and buncher trap (RFCT), an electron beam ion trap (EBIT for charge breeding) and a Penning trap (MPET) (Fig.7). Their prime application is the high-precision mass measurements of short-lived isotopes [60], however, the versatility of the ion trap manipulation and storage technique allows also other applications.

At ISAC, the radioactive isotopes are produced by bombarding a thick target with 500 MeV protons at intensities of up to 75 μA [61]. Reaction products diffuse out of the traget, are being ionized and electrostatically accelerated up to 60 keV. The so-formed beam is mass separated and delivered to the ISAC experiments, one of which is TITAN. The beam enters the gas-filled RFQ, where it is being cooled and bunched, and then transferred to the next component. In the present setup for EC measurements, the beam is then transferred to the Measurement Penning Trap (MPET), where mass selective buffer gas cooling will be carried out. This is an established technique [62,63] and requires bleeding of a small amount of buffer gas at a level of $p_{\rm trap} \approx 10^{-6}$ mbar into the Penning trap. Collisions of stored ions with the inert gas atoms will lead to cooling and thermalization. In order to keep the ions confined to the center of the trap, a quadrupolar RF-field is applied. Its frequency is mass dependent and allows a clean selection of the isotopes under consideration. Ion masses which do not match the RF-frequency will quickly leave the trap center and will be lost due to collisions with the trap electrodes [62]. Figure 8 shows a mass scan from the ISOLTRAP collaboration [64], where an on-line cocktail beam could be separated with a mass resolving power of 50,000. A resolving power between 10^4 and $2 \cdot 10^5$ for an ion beam of mass $A \sim 100$ was recently achieved with the JYFLTRAP system [65] by employing this mass selective buffer gas cooling technique.

The purified sample then enters the EBIT [66, 67]. The EBIT will be used in a so-called Penning-trap mode, i.e. without the application of the electron beam. The charged ions will be trapped and stored by the super-conducting 6T magnetic field and by the electrostatic potentials applied to the trapping electrodes. The EBIT is operated in a 'cold-bore' configuration, i.e. the electrodes are at LHe temperature. The vacuum in the system is good enough to reach trapping times on the order of

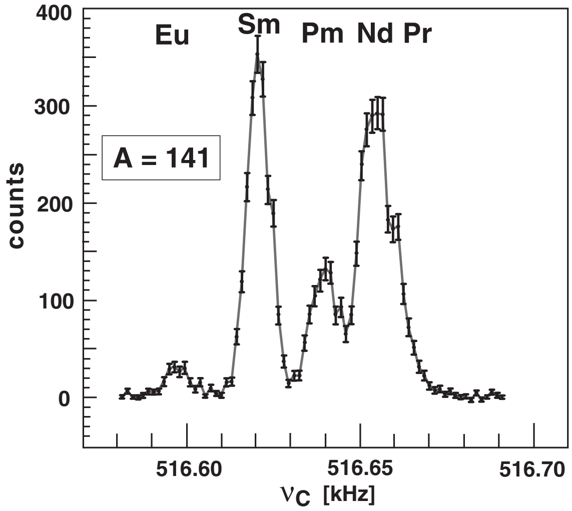

Fig. 8. Mass scan example from the ISOLTRAP experiment [64]. The individual isobars at mass $\mathrm{A} = 141$ are cleanly resolved. The quoted resolving power was $R > 50,000$.

minutes or more ($p_{\mathrm{EBIT}} \approx 1 \cdot 10^{-11}$ mbar). The magnet system used for the EBIT is a Helmholtz coil configuration and provides easy access to the center of the trap. The geometry of the EBIT is shown in Fig.9. The EBIT will provide ideal storage conditions for the radioactive ion sample. Its geometry allows for X-ray detectors to be mounted close to the center of the trap, which is a unique characteristic of the system. An additional β^{-}-counter can be inserted in the vacuum cross, because once the electron gun (E-gun) is fully retracted, this space becomes available. The E-gun is mounted on a linear feed-thru, and can be pulled sufficiently far back as to not interfere with the rest of the setup.

The seven detectors can detect the emitted X-rays without interference from electrons emitted by the much more intense β-decay. The β-decay electrons will be guided by the magnetic field lines away from the X-ray detectors and focused to the axis of the magnet at the exit. There they can be observed with a suitable detector placed on axis, though still within the high field region of the magnet. The detection would operate in anti-coincidence in order to gate on possible X-rays which are associated with the β-decay. The detector will either be a micro-channel-plate detector, or a channeltron, both of which are known to operate in high magnetic fields [68, 69].

For an absolute branching ratio measurement, the total number of ions in the sample need to be determined. This can be done in batch-mode operation. A first batch will be prepared as an isotopically pure sample, trapped in the EBIT and expelled onto an ion detector (or the same β-detector) for counting. This determines the number of ions per spill. The following number of on-line produced ions in each batch can then be monitored via the detected electrons. Well established EC rates can be used as calibration points for total detection efficiencies.

4. Conclusion

Double-beta decay is presently at the forefront of experimental research in sub-atomic physics. This is because the mere observation of the $0\nu\beta\beta$-decay mode would immediately signal physics beyond the Standard Model as it implies the neutrino to be a Majorana particle. However, when attempting to extract the mass of the neutrino from a particular decay – once it is observed –, the poor knowledge of the nuclear physics constitutes an almost embarrassing situation. None of the nuclear matrix elements

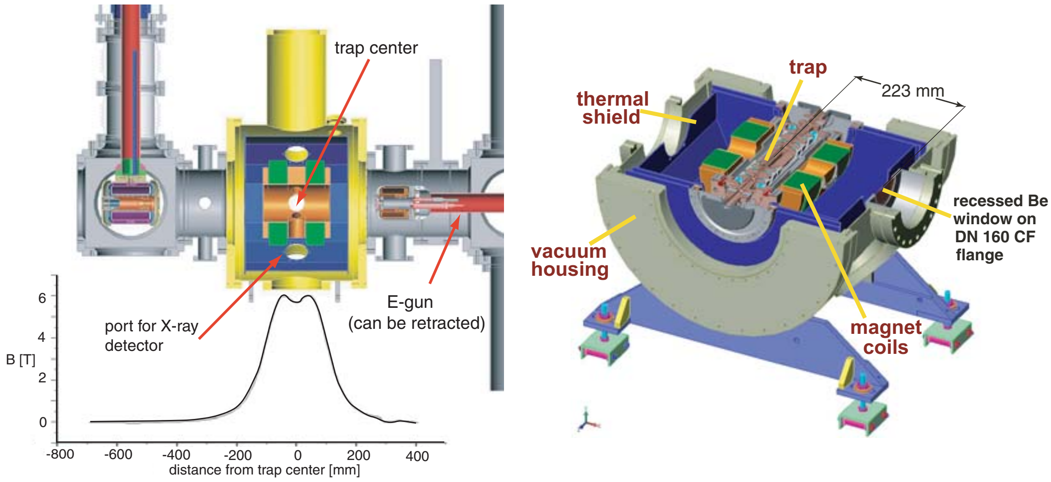

Fig. 9. Left: EBIT schematic setup together with magnetic field distribution. The E-gun head will be retracted to make room for a β-counter. Right: Cross sectional view of the trap showing the position of the Be-windows. A modification to re-position the windows further inside to increase the solid angle is mechanically possible, but requires a modification of the cryogenic part.

needed for this seems to have a solid experimental foundation. In this paper we have addressed this deficiency and given ideas on how to improve our knowledge by applying a novel technique using the TITAN ion trap facility in conjunction with the TRIUMF ISAC radioactive beams. We have shown that the technique has the potential for precision measurements of EC ratios for allowed and first-order forbidden decays from ground states or from isomeric states of the intermediate odd-odd nuclei and thereby significantly contribute to the knowledge of nuclear matrix elements involved. We have further shown that charge-exchange reactions like (d,^{2}He) and (^{3}He,t) can probe the Gamow-Teller matrix elements at higher excitations. This was exemplified by new results from a ^{76}Se(d,^{2}He)^{76}As experiment performed at an intermediate energy of 183 MeV. In view of the upcoming initiatives of measuring $\beta\beta$-decay in many different systems, a concerted theoretical and experimental effort is needed to address the important issue of the $\beta\beta$-decay nuclear matrix elements.

5. Appendix

When comparing numbers, units often turn out to be a source of confusion. In this paper, $B(GT)$ values are given in units in which the neutron decay has $B(GT) = 3$. Further,

$$B(GT) = \frac{1}{2J_i + 1}|M(GT)|^2 = \frac{1}{2J_i + 1}|\langle f \| \sum_k \sigma^k \tau^k_\pm \| i \rangle|^2, \tag{5.1}$$

with $M(GT)$ the nuclear matrix element. Spin factors must be taken into account, but the presently quoted $B(GT)$ values always refer to the $0^+ \longrightarrow 1^+$ transitions among the involved isobars (which is usually the direction of charge-exchange reaction). The connection between the ft value and $B(GT)$ is [70, 71]:

$$ft = \frac{(6146 \pm 6)\ [s]}{g_A^2 B(GT)}\ , \tag{5.2}$$

with $g_A = -1.257$ being the free nucleon axial vector coupling constant. For the evaluation of $log\ ft$-values, we use the compilation of Gove and Martin [49] from 1971. In some cases we find differences to previously published EC $log\ ft$-values. We have not tried to find the sources of these discrepancies. All isotopic information was retrieved from Ref. [72], unless otherwise stated.

6. Acknowledgement

The ideas to this paper were conceived during DF's extended stay at TRIUMF, and he wishes to express his deepest appreciation and gratitude to the Directorate at TRIUMF for all the support he has enjoyed during this stay. Many people at TRIUMF and elsewhere have contributed in one or the other way to various aspects of the present study, which eventually has led to an experimental proposal (TR-1066) at TRIUMF. The authors wish to express their gratitude to all of them.

References

1. G. Prezeau, M. Ramsey-Musolf and P. Vogel, Phys. Rev **D68**, 034016 (2003).
2. V. Cirigliano, A. Kurylov, M. J. Ramsey-Musolf and P. Vogel, Phys. Rev. **D70**, 075007(2004).
3. V. Cirigliano, A. Kurylov, M. J. Ramsey-Musolf and P. Vogel, Phys. Rev. Lett. **93**, 231802 (2004).
4. H. Primakoff and S. P. Rosen, Rep. Prog. Phys. **22**, 121 (1959).
5. J. Suhonen and O. Civitarese, Phys. Rep. **300**, 123 (1998).
6. S. Rakers, C. Bäumer, A. M. van den Berg, B. Davids, D. Frekers, D. De Frenne, Y. Fujita, E.-W. Grewe, P. Haefner, M. N. Harakeh, M. Hunyadi, E. Jacobs, H. Johansson, B. C. Junk, A. Korff, A. Negret, L. Popescu, H. Simon, and H. J. Wörtche, Phys. Rev. **C70**, 054302 (2004).
7. S. Rakers, C. Bäumer, A. M. van den Berg, B. Davids, D. Frekers, D. De Frenne, E.-W. Grewe, P. Haefner, M. N. Harakeh, S. Hollstein, M. Hunyadi, E. Jacobs, B. C. Junk, A. Korff, A. Negret, L. Popescu, and H. J. Wörtche, Phys. Rev. **C71**, 054313 (2005).
8. H. Ejiri, Phys. Rep. **338**, 265 (2000), and Journ. Phys. Soc. Japan **74**, 2101 (2005).
9. W. P. Alford and B. Spicer, Adv. Nucl. Phys. **24**, 1 (1994).
10. W. P. Alford, R. L. Helmer, R. Abegg, A. Celler, D. Frekers, P. Green, O. Häusser, R. Henderson, K. Hicks, K. P. Jackson, R. Jeppeson, C. A. Miller, A. Trudel, M. Vetterli, S. Yen, R. Pourang, J. Watson, B. A. Brown and J. Engel, Nucl. Phys. **A514**, 49 (1990).
11. T. N. Taddeucci, C. A. Goulding, T. A. Carey, R. C. Byrd, C. D. Goodman, C. Gaarde, J. Larsen, D. Horen, J. Rapaport, E. Sugarbaker, Nucl. Phys. **A469**, 125 (1987).
12. B. D. Anderson, T. Chittrakarn, A. R. Baldwin, C. Lebo, R. Madey, P. C. Tandy, J. W. Watson, B. A. Brown and C. C. Foster, Phys. Rev. **C31**, 1161 (1985).
13. C. D. Goodman, C. A. Goulding, M. B. Greenfield, J. Rapaport, D. E. Bainum, C. C. Foster, W. G. Love and F. Petrovich, Phys. Rev. Lett. **44**, 1755 (1980).
14. J. Schlechter and J. W. F. Valle, Phys. Rev **D25**, 2951, (1982).
15. J. Suhonen, S. B. Khadkikar and A. Faessler, Phys. Lett. **237B**, 8 (1990).
16. J. Suhonen, S. B. Khadkikar and A. Faessler, Nucl. Phys. **A529**, 727 (1991).
17. J. D. Vergados, Nucl. Phys. **A506**, 482 (1990).
18. J. Suhonen, Phys. Lett. **607B**, 87 (2005).
19. O. Civitarese and J. Suhonen, Phys. Lett. **626B**, 80(2005).
20. H. Muto, Phys. Lett. **B391**, 243 (1997).
21. M. Aunola and J. Suhonen, Nucl. Phys. **A643**, 207 (1998).
22. S. Stoica and H. V. Klapdor-Kleingrothaus, Phys. Rev. **C63**, 064304 (2001).
23. S. Stoica and H. V. Klapdor-Kleingrothaus, Nucl. Phys. **A694**, 269 (2001).
24. V. A. Rodin, A. Faessler, F. Šimkovic and P. Vogel, Phys. Rev. **C68**, 044302 (2003).
25. V. A. Rodin, A. Faessler, F. Šimkovic and P. Vogel, Nucl. Phys. **A766**, 107 (2006).
26. F. Šimkovic, A. A. Raduta, M. Veselsky, and A. Faessler, Phys. Rev. **C61**, 044319 (2000).
27. R. Álvarez-Rodríguez, P. Sarriguren, E. Moya de Guerra, L. Pacearescu, A. Faessler, and F. Šimkovic, Phys. Rev. **C70**, 64309 (2004).
28. K. Zuber, Summary of Workshop on Nuclear Matrix Elements for Neutrinoless Double-beta Decay, Inst. F. Part. Phys. Phen. Univ. Durham, UK, June-2005 and preprint nucl-ex/0511009.

29. H. Akimune, H. Ejiri, M. Fujiwara, I. Daito, T. Inomata, R. Hazama, A. Tamii, H. Toyokawa, and M. Yosoi, Phys. Lett. **394B**, 23 (1997).
30. M. Bhattacharya, A. García, M. M. Hindi, E. B. Norman, C. E. Ortiz, N. I. Kaloskamis, C. N. Davids, O. Civitarese, and J. Suhonen, Phys. Rev. **C58**, 1247 (1998).
31. Sam M. Austin, N. Anantaraman, and W. G. Love, Phys. Rev. Lett. **73**, 30 (1994).
32. H. V. Klapdor-Kleingrothaus , I. V. Krivosheina , A. Dietz and O. Chkvorets, Phys. Lett. **586B**, 198 (2004).
    H. V. Klapdor-Kleingrothaus , A. Dietz , I. V. Krivosheina and O. Chkvorets, Nucl. Instrum. Methods Phys. Res., Sect. **A 522**, 371 (2004).
33. M. O. Krause, J. Phys. Chem. Ref. Data **8**, 307 (1979).
34. A. García, Y-D Chan, M. T. F. da Cruz, R. M. Larimer, K. T. Lesko, E. B. Norman, R. G. Stokstad, F. E. Wietfeldt, I. Žlimen, D. M. Moltz, J. Batchelder, and T. J. Ognibene,Phys. Rev. **C47**, 2910 (1993).
35. H. Ejiri, J. Engel, R. Hazama and P. Krastev, Phys. Rev. Lett. **85**, 2917 (2000).
    H. Ejiri, Phys. Rep. **338**, 265 (2000).
    H. Ejiri, J. Engel, K. Fushime and K. Hayashi, Nucl. Phys. B Proc. Suppl. **110**, 375 (2002).
    H. Ejiri, J. Engel and N. Kudomi, Phys. Lett. **530B**, 27 (2002).
    P. Doe, H. Ejiri, S. R. Elliott and J. Engel, Nucl. Phys. **A721** (2003) 517c.
    R. Hazama, P. Doe, H. Ejiri and S.R. Elliott, Nucl. Phys. B Proc. Suppl. **138**, 102 (2005).
    H. Nomachi, P. Doe, H. Ejiri and S.R. Elliott, Nucl. Phys. B Proc. Suppl. **138**, 221 (2005).
36. B. Singh and J. A. Szucs, Nucl. Data Sheets **60**, 1 (1990).
37. H. Ejiri, K. Fushimi, T. Kamada, H. Kinoshita, H. Kobiki, H. Ohsumi, K. Okada, H. Sano, T. Shibata, T. Shima, N. Tanabe, J. Tanaka, T. Taniguchi, T. Watanabe and N. Yamamoto, Phys. Lett. **258B**, 17 (1991).
38. H. Ejiri, K. Higa, T. Kamada, H. Kobiki, K. Matsuoka, K. Okada, H. Sano, T. Shibata, T. Shima, N. Tanabe, J. Tanaka, T. Taniguchi, T. Watanabe and N. Yamamoto, Nucl. Instrum. Methods Phys. Res., Sect. **A 302**, 304 (1991).
39. R. Arnold, C. Augier, A. M. Bakalyarov, J. Baker, A. Barabash, Ph. Bernaudin, M. Bouchel, V. Brudanin, A. J. Caffrey, J. Cailleret, J. E. Campagne, D. Dassié, V. Egorov, K. Errahmane, A. I. Etienvre, T. Filipova, J. Forget, A. Guiral, P. Guiral, J.L. Guyonnet, F. Hubert, Ph. Hubert, B. Humbert, R. Igersheim, P. Imbert, C. Jollet, S. Jullian, I. Kisel, A. Klimenko, O. Kochetov, V. Kovalenko, D. Lalanne, F. Laplanche, B. Lavigne, V. I. Lebedev, J. Lebris, F. Leccia, A. Leconte, I. Linck, C. Longuemare, Ch. Marquet, G. Martin-Chassard, F. Mauger, I. Nemchenok, I. Nikolic-Audit, H. Ohsumi, S. Pécourt, F. Piquemal, J. L. Reyss, A. Richard, C. L. Riddle, J. Rypko, X. Sarazin, L. Simard, F. Scheibling, Yu. Shitov, A. Smolnikov, I. Štekl, C. S. Sutton, G. Szklarz, V. Timkin, V. Tretyak, V. Umatov, L. Vála, I. Vanushin, S. Vasiliev, V. Vasilyev, V. Vorobel, Ts. Vylov, J. Wurtz and S. V. Zhukov, Nucl. Instrum. Methods Phys. Res., Sect. **A 536**, 79 (2005).
40. R. Arnold, C. Augier, J. Baker, A. Barabash, G. Broudin, V. Brudanin, A. J. Caffrey, E. Caurier, V. Egorov, K. Errahmane, A. I. Etienvre, J. L. Guyonnet, F. Hubert, Ph. Hubert, C. Jollet, S. Jullian, O. Kochetov, V. Kovalenko, S. Konovalov, D. Lalanne, F. Leccia, C. Longuemare, G. Lutter, Ch. Marquet, F. Mauger, F. Nowacki, H. Ohsumi, F. Piquemal, J. L. Reyss, R. Saakyan, X. Sarazin, L. Simard, F. Šimkovic, Yu. Shitov, A. Smolnikov, L. Štekl, J. Suhonen, C. S. Sutton, G. Szklarz, J. Thomas, V. Timkin, V. Tretyak, V. Umatov, L. Vála, I. Vanushin, V. Vasilyev, V. Vorobel, and Ts. Vylov, Phys. Rev. Lett. **95**, 182302 (2005).
41. F. Šimkovic, G. Pantis, J. D. Vergados and A. Faessler, Phys. Rev. **C60**, 055502 (1999).
42. J. Suhonen and M. Aunola, Nucl. Phys. **A723**, 271 (2003).
43. J. Wilkerson, preliminary results presented at the International Workshop on Neutrino Nuclear Responses in Double Beta Decays and Low-energy Astro-neutrinos (NNR05), Dec. 2-4, 2005, CAST/Spring-8, Japan.
44. H. Ejiri, Prog. in Part. and Nucl. Phys. **40**, 307 (1998).
45. J. Blachot and G. Marguier, Nucl. Data Sheets **60**, 139 (1990).
46. J. Blachot and G. Marguier, Nucl. Data Sheets **73**, 81 (1994).
47. L. Frevert, R. Schöneberg and A. Flammersfeld, Zeit. f. Physik **182**, 439 (1965) (in German).
48. L. Grodzin and H. Motz, Phys. Rev. **102**, 761 (1956).
49. N. B. Gove and M. J. Martin, Nucl. Data Tables **10**, 205 (1971).
50. N. Benczer B. Farrelly, L. Koerts and C. S. Wu, Phys. Rev. **101**, 1027 (1956).

51. E. W. Schneider, M. D. Glascock, W. B. Walters and R. A. Meyer, Phys. Rev. **C19**, 1025 (1979).
52. K. Zuber, Phys. Lett. **519B**,1 (2001).
    H. Kiel, D. Münstermann and K. Zuber, Nuclear Physics **A723**, 499 (2003).
53. C. Arnaboldi, F. T. Avignone III, J. Beeman, M. Barucci, M. Balata, C. Brofferio, C. Bucci, S. Cebrian, R. J. Creswick, S. Capelli, L. Carbone, O. Cremonesi, A. de Waard, E. Fiorini, H. A. Farach, G. Frossati, A. Giuliani, P. Gorla, E. E. Haller, I. G. Irastorza, R. J. McDonald, A. Morales, E. B. Norman, A. Nucciotti, M. Pedretti, C. Pobes, V. Palmieri, M. Pavan, G. Pessina, S. Pirro, E. Previtali, C. Rosenfeld, S. Scopel, A. R. Smith, M. Sisti, G. Ventura and M. Vanzini, Astropart. Phys. **20**, 91 (2003).
    C. Arnaboldi, F. T. Avignone III, J. Beeman, j, M. Barucci, M. Balata, C. Brofferio, C. Bucci, S. Cebrian, R. J. Creswick, S. Capelli, L. Carbone, O. Cremonesi, A. de Ward, E. Fiorini, H. A. Farach, G. Frossati, A. Giuliani, D. Giugni, P. Gorla, E. E. Haller, I. G. Irastorza, R. J. McDonald, A. Morales, E. B. Norman, P. Negri, A. Nucciotti, M. Pedretti, C. Pobes, V. Palmieri, M. Pavan, G. Pessina, S. Pirro, E. Previtali, C. Rosenfeld, A. R. Smith, M. Sisti, G. Ventura, M. Vanzini and L. Zanotti, Nucl. Instrum. Methods Phys. Res., Sect. **A 518**, 775 (2004).
54. J. Scobie, Nucl. Phys. **3**, 465 (1957).
55. H.-V. Klapdor-Kleingrothaus, A. Dietz, H. L. Harney and I. V. Krivosheina, Mod. Phys. Lett. **A16** 2409 (2001).
56. P. Peiffer, D. Motta, S. Schoenert and H. Simgen, Nucl. Phys. Proc. Suppl. **B143**, 511 (2005).
    I. Abt, M. Altmann, A. Bakalyarov and I. Barabanov, hep-ex/0404039, GERDA proposal submitted to Gran Sasso Scientific Committee.
57. C. E. Aalseth, D. Anderson, R. Arthur and F.T. Avignone III, Nucl. Phys. B, Proc. Suppl. **138**, 217, (2005).
    C. E. Aalseth, D. Anderson, R. Arthur and F. T. Avignone III, Physics of Atomic Nuclei, **67**, 2002, (2004).
58. For information refer to the following URL http://www.snolab.ca
59. E. Caurier, F. Nowacki, A. Poves and J. Retamosa, Phys. Rev. Lett. **77**, 1954 (1996).
60. J. Dilling, P. Bricault, M. Smith, H.-J. Kluge and TITAN collaboration, Nucl. Instrum. Methods Phys. Res., Sect. **B204**, 492 (2003)
61. M. Dombsky, R. Baartman, P. Bricault, J. Doornbos, P. Bricault, J. Doornbos, K. Jayamanna, T. Kuo, G. Mackenzie, M. McDonald, P. Schmor and D. Yuan, Proc. 7^{th} Int. Conf. on Ion Sources (Taormina, Italy, 1997), Rev. Sci. Instrum. **69**, 1170 (1998)
    T. Kuo, D. Yuan, K. Jayamanna, M. McDonald, R. Baartman, G. Mackenzie, P. Bricault, M. Dombsky, P. Schmor and G. Dutto, Proc. 7^{th} Int. Conf. on Ion Sources (Taormina, Italy, 1997), Rev. Sci. Instrum. **69**, 767 (1998).
62. G. Savard, St. Becker, G. Bollen and H. -J. Kluge, Phys Lett. **158A**, 247 (1991).
63. V. S. Kolhinen, S. Kopecky, T. Eronen, U. Hager, J. Hakala, J. Huikari, A. Jokinen, A. Nieminen, S. Rinta-Antila, J. Szerypo and J. Äystö, Nucl. Instrum. Methods Phys. Res., Sect. **A528**, 776 (2004).
64. H. Raimbault-Hartmann, D. Beck, G. Bollen, M. König, H.-J. Kluge, E. Schark, J. Stein, S. Schwarz and J. Szerypo, Nucl. Instrum. Methods Phys. Res., Sect. **B126**, 378 (1997).
65. S. Rinta-Antila, S. Kopecky, V. S. Kolhinen, J. Hakala, J. Huikari, A. Jokinen, A. Nieminen, and J. Äystö, Phys. Rev. **C70**, 011301R (2004).
66. G. Sikler, J. R. Crespo López-Urrutia, J. Dilling, S. Epp, C. J. Osborne and J. Ullrich, Euro. Phys. J. **A25** ,s01, 63 (2005).
67. J. Dilling, R. Baartman, P. Bricault, M. Brodeur, L. Blomeley, F. Buchinger, J. Crawford, J. R. C. López-Urrutia, P. Delheij, M. Froese, G. P. Gwinner, Z. Ke, J. K. P. Lee, R. B. Moore V. Ryjkov, G. Sikler, M. Smith, J. Ullrich and J. Vaz, International Journal of Mass Spectrometry, **251**, 198 (2006).
68. G. W. Fraser and J. F. Pearson, Nucl. Instrum. Methods Phys. Res., Sect. **A293**, 569 (1990).
69. A. Tremsin, J. F. Pearson, G. W. Fraser, W. B. Feller and P. White, Nucl. Instrum. Methods Phys. Res., Sect. **A379**, 139 (1996).
70. G. Martínez-Pinedo, A. Poves, E. Caurier, and A. P. Zuker, Phys. Rev. C **53**, R2602 (1996).
71. I. S. Towner and J. C. Hardy, nucl-th/9504015 (1995).
72. R. B. Firestone, V. S. Shirley, C. M. Baglin, J. Zipkin and S. Y. F. Chu, Table of Isotopes CD-ROM, Eighth Edition, Vers. 1.0, (1996).